Vol.3 No.1 Jan 2020

Journal of Computational Mechanics, Power System and Control

Received 7 October, Revised 29 November, Accepted 29 December

Black Widow Optimization Algorithm: Optimal Designing and modelling and of LLC Resonant Converter

Sarath K S
Hindustan University
Padur, Chennai, India
sarathksks6@gmail.com

Sekar S
Department of Electrical Electronics Engineering
Hindustan University
Padur, Chennai, India

Abstract: In the 80s, Resonant Converter (RC) was created under analysis extensively that can reach a minimum loss of switching, hence, ease resonant topologies to work in the maximum switching frequency. In the state of the arts, it is well discussed that the optimal parameterization of the RC is a vital assignment. While the state of the arts has dealt with the diverse technologies, they are extremely theoretical and as a result, the uncertainty because of high hypothetical effect persists. The prime intention of this work is to develop an optimization technique for developing and designing of LLC-RC. The proposed technique overcomes the restriction by developing a non-theoretical technique on the basis of the experimented result. Especially, the under start-up circumstances, the resonant current is obtained from the state-of-the-art result, and the intelligent technique is modeled. On the basis of the proposed technique, a well-known optimization approach known as Black Widow Optimization Algorithm (BWOA) is used for the optimization of the time constant for the RC that is a serious parameter of the design. The objective function is devised as a model of start-up time therefore the start-up time able to reduce. Furthermore, the response speed of the output voltage is maximized. The proposed BWOA is evaluated with the existing models and the attained consequence confirms the operation of the proposed model in designing the LLC-RC model.

Keywords: LLC RC; Startup Process; Output Voltage; Peak Value; Black Widow; Optimization Algorithm

Nomenclature

Abbreviations	Descriptions
RC	Resonant Converters
UPS	Uninterrupted Power Supply
DCTs	DC Transformers
ZCS	Zero Current Switching
HB	Half Bridge
FHA	Fundamental Harmonic Approximation
ZVS	Zero Voltage Switching
SST	Solid-State Transformer
DB	Dual-Bridge
FB	Full-Bridge
CR	Cannibalism Rating

1. Introduction

By means of the modern advancement of telecommunications and electronic technologies, emerges an obligation which leads the prosperity, of reducing the apparatus, when retaining a significant performance [1]. The integration of these features consequences in a significant power density apparatus that is the preferred objective. Nevertheless, a large number of electronic functions operate with distinct voltage standards which do not symbolize the voltage turned over using the source, generally a battery otherwise using the electric grid via an AC-DC converter. This affirms the usefulness of a DC-DC converter to revise the power supply to the loads.

RC is presented with the primary intention of augmenting the power density, by minimizing the volume of factors, employing a large operating frequency, and reducing the losses of switching. At a

https://doi.org/10.46253/jcmps.v3i1.a4

frequency, their working rule comprises stimulating an LC circuit adjacent to its resonant frequency with the intention of oscillating the current or voltage in the devices, switching them at the zeros of their current or voltage, pointed to zero switching losses, relatively. Nevertheless, in recent years the possibility of the RC to reach both significant capability and significant power density experiences managed to a comprehensive research, accordingly, it is prerequisite that the techniques utilized in the investigation and model of these converters are as identical as feasible or, if not so, which the error suggested by them is evaluated and reported [20].

The LLC RC erstwhile extensively employed in the server power supply, electric vehicle charger, and UPS circumstances for its benefits, like isolation, high-efficiency soft switching, adjustable voltage, and high switching frequency [5]. In the standard instance, the magnetizing inductance, resonant inductance, and resonant capacitance, work simultaneously to obtain the transfer of energy. With half duty cycle, frequency modulation control is constantly developed. In addition, while the switching frequency is flatter than the resonant frequency, ZVS turn-on of primary-side switches and ZCS turn-of rectifier diodes can be attained [5].

In the past, various design techniques have been established. They can be encapsulated into three sections such as a) FHA b) FHA with time-domain correction, and c) time-domain analysis. In [5], a crucial observation is explained which though 3 values of factor are to be performed, the aspects of an LLC converter are worked out by merely 2 variables: the ratio of inductance and the quality factor of the resonant tank. While these 2 variables are preferred, yet at specific frequencies of resonant, the LLC converters will encompass a similar peak increase.

Usually, for LLC, preceding design techniques converters employ the peak gain obligation and added circumstances to develop a model, like operation at no load [7] predefined dead time length [8], short-circuit operation [13], soft start inrush current [9], maximum resonant capacitor voltage [10], secondary-side leakage inductance [11], normalized switching frequency range [12], and etc. Nevertheless, while the model intention is a performance optimization, these added conditions put needless constraints and eliminate potential model candidates.

The main contribution of this paper is to introduce a novel approach called as Black Widow Optimization Algorithm in order to model for LLC-RC by optimizing the resonant inductor current and output voltage, therefore, the error can be reduced. The proposed algorithm is evaluated with conventional techniques so as to examine the enactment of the developed model with conventional techniques.

2. Literature Review

In 2019, Siniša Zorica et al [1] developed on the design of the preferred converter working area in the ratio of the DC conversion feature and the computation of rates for component exploiting parameters, which obtain from the chosen working region. In Mode I, the realized converter prototype works with high full load competence. The significant incomplete load competence was preserved downward to 50% of the complete load. With small frequency switching alters; the realized converter preserves a constant current output. For both the diodes rectifier and power switches, the zero voltage switching was attained via the load range.

In 2018, Chuang Liua et al [2] developed a novel breed of SST distribution tail method mostly on the basis of DC-DC RC and hybrid multilevel cascaded converter among the minimum voltage customer side and medium-voltage distribution. The developed SST topology mostly integrates per-phase H-bridge cascaded converters on the basis of the DCTs with the square-wave 2-level VSC on the basis of the collect DCT together. In the quasi-resonant mode, for the medium voltage side, the developed model can present the equipped pliability for reactive and active power control on the basis of the cut down single-stage control system arrangement idea because of the features of the resonant DC-DC converters functioning.

In 2018, Chih-Chiang Hua and Yung-lin Deng [3] developed a DB LLC RC method with a broad area of minimum input voltage for dc/dc conversion. The developed converter front phase was on the basis of the switch incorporation method, which combines the buck-boost converter with the HB LLC and FB LLC at the front phase as a novel single-phase DB LLC. Additionally, the model of the inductance of magnetizing was increased. At varying input voltages, the DB LLC RC exploits various phase-shift modulations that increase MD in order to simply attain an extensive input voltage series with merely small alterations in frequency. Lastly, at diverse light load circumstances, diverse actual duty ratios were presented to achieve less power loss. Hence, the developed model possesses maximum effectiveness at light load circumstances and its voltage regulation was minimized.

In 2018, Dongjiang Yang et al [4], suggested the LLC-C converter, for each resonant capacitor, two auxiliary switches were augmented to give a bypass path. The converter can function as a conventional LLC RC that includes further techniques to design and analysis in either backward or forward operating procedure. Additionally, a model procedure was suggested in order to model the LLC-C converters in a most favorable way.

In 2019, Fang Li et al [5], worked on the LLC RC, which was extensively exploited in Direct Current– Direct Current conversion technologies. Nevertheless, the parasitic modules of the LLC RC had an important effect in sensible pieces of equipment, like on the conduction loss influence and the power devices soft-switching, the oscillation of voltage athwart diodes of the rectifier, and during light load circumstance the unfettered output voltage, etc. For the higher-order circuits, it was difficult to evaluate using the existing study techniques. Concentrating at the LLC converter operational rule with the parasitic module, the differential equation system was developed.

In 2018, Arief Noor Rahman et al [6], worked on the resonant circuit that was extensively developed to attain high conversion competence using soft switching for the power transistor. Usually, the majority deployed RC was series RC because of its usual potential for the process of bidirectional power flow, easy design and process in bidirectional converter application. Nevertheless, for bidirectional operation, a series RC operating gain range was restricted to utmost at unity, ensuing in complexity controlling the output voltage. For the bidirectional process to enhance the regulation of the output voltage, the LLC resonant tank was chosen as an attractive option to SRC resonant tank. In a bidirectional converter application exploiting LLC resonant tank, it needs two diverse operation modes based upon the direction of power flow.

3. LLC Resonant Converter Modeling

The LLC-RC experiences turned into a convenient topography for enhanced power density, and a great performance of DC-DC converter in addition to various functions is worked out on the basis of this technique for significant developments. Frequency modulation control is broadly approved also preferred option to carry out clearer the control system and get the measurements in real-time, from exact high frequency f_{st} it decides the switching that mitigates in an exponential otherwise linear pattern to steady-state frequency f_r, that is $f = f_r + (f_{st} - f_r)e^{\frac{-t}{\tau}}$ as demonstrated in Fig. 1, whereas τ indicates frequency time constant and t indicates time. The exponential delineate is simple, which needs to deal with a first-order filter, and while switching it obtains additional smooth frequency conversion. Conversely, the trial, and error model recitation, τ is tiresome [14], because of the absence in the accurate examination of the dynamic process of the converter.

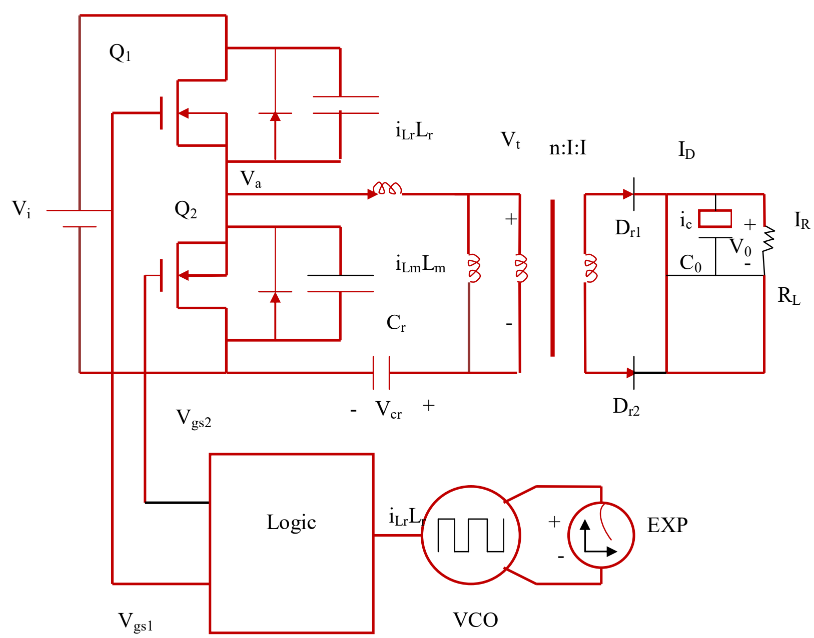

Fig. 1. *Block diagram of LLC-RC*

3.1. STARTUP Procedure and Optimization of Parameters

On the basis of the integrated state formulations, the radius, and centre of trajectory of arc, is often related to the voltage of the output. Through the start-up, the complete state variables can be carried out if it controls the output voltage.

3.1.1 Output Voltage Measurement

The current rectifier is referred to as assist the capacitor charging power, in order to decrease the load current. At the output the capacitor is enormous adequate, it can deal with the output voltage during half a switching period with as stable, hence does the load current. As in eq.(1), during the output, augmented voltage at one observed period of the rectifier, whereas i_c indicates the capacitor current, i_R indicates load current, i_D indicates the summation of the current of two rectifier diodes, and C_0 indicates output current.

$$\Delta V_0 = \frac{1}{C_0}\int_0^{\frac{T_s}{2}} i_c dt = \frac{1}{C_0}\int_0^{\frac{T_s}{2}} (i_D - i_R)dt \tag{1}$$

Subsequently, at the output i_c, the mean value of the capacitor current and the summation of magnetic current, which is symmetrical i_{Lm} and it is approximately equal to "0" in a steady state of the single conducting period for the rectifier, therefore eq. (2) is devised.

$$n\int_0^{\frac{T_s}{2}} i_{Lr} dt \frac{V_0 T_s}{2R_L} = 0 \tag{2}$$

Throughout a conducting period of the rectifier, eq. (3) and eq. (4) are devised which varies from $t1$ to $t3$,

$$\int_0^{\frac{T_s}{2}} i_{Lr} dt = \int_0^{\frac{T_s}{2}} C_r \frac{dv_{C_r} dt}{dt} = C_r\left(V_{C_{r3}} - V_{C_{r1}}\right) \tag{3}$$

$$\Delta V_0 = \frac{nC_r(V_{Cr3} - V_{Cr1})}{C_0} - \frac{V_0 T_s}{2R_L C_0} \tag{4}$$

In Eq. (3), C_r indicates the capacitor resonant, V_{C_r} indicates the capacitor resonant voltage, R_L indicates the significant resistor load, Z_0 states the resonant impedance, i_{Lr} states the inductor resonant current and T_s states the switching period.

Taking into consideration of eq. (5), eq. (6) is devised, where ϕ_1 and ϕ_2 are the main phases related to the center of the arc $(x_1,0)$ and $(x_2,0)$ at t_1 and t_2 individually as stated in eq. (6). In eq. (5) and Eq. (6), ω_0 indicates the natural frequency $\left(\omega_0 = \frac{1}{\sqrt{L_r C_r}}\right)$.

$$\begin{cases} i_{Lr1} = I_{Lrp1}\sin(\omega_0 t + \varphi_1)\big|_{mode1} \\ i_{Lr2} = I_{Lrp2}\sin(\omega_0 t + \varphi_2)\big|_{mode2} \end{cases} \tag{5}$$

$$\begin{cases} I_{Lrp1} = \sqrt{\dfrac{(V_{Cr1} - x_1)^2}{Z_0^2 + (-I_{Lm})^2}} \\ I_{Lrp2} = \sqrt{\dfrac{(V_{Cr2} - x_2)^2}{Z_0^2 + (-I_{Lr})^2}} \\ V_{Cr2} = I_{Lrp1} Z_0 \cos(\omega_0 t_{12} + \varphi_1) + x_1 \end{cases} \tag{6}$$

As demonstrated in eq. (7), in the inductor, the current is balanced whereas I_{Lm} indicates the exhilarating current.

$$\begin{cases} I_{Lrp1}\sin\varphi_1 = -I_{Lm} \\ I_{Lr2} = I_{Lrp1}\sin(\omega_0 t_{12} + \varphi_1) = I_{Lrp2}\sin\varphi_2 \\ I_{Lrp1}\sin(\omega_0 t_{23} + \varphi_2) = I_{Lm} \end{cases} \tag{7}$$

The time among t_{01} and t_{02} equivalent to half a switching period, in that t_{01} indicates the freewheeling instance for the rectifier diode, which is equal to $t_{23-last}$, the freewheeling instance of the preceding form of the performance. Hence, the whole variables are attained, V_{Cr3} is also estimated as ΔV_0. Fig 2 states the flow chart of the state variable measurement.

$$t_{01} + t_{02} = \frac{T_s}{2} \tag{8}$$

$$V_{Cr3} = I_{Lrp2} Z_0 \cos(\omega_0 t_{23} + \varphi_2) + x_2 \tag{9}$$

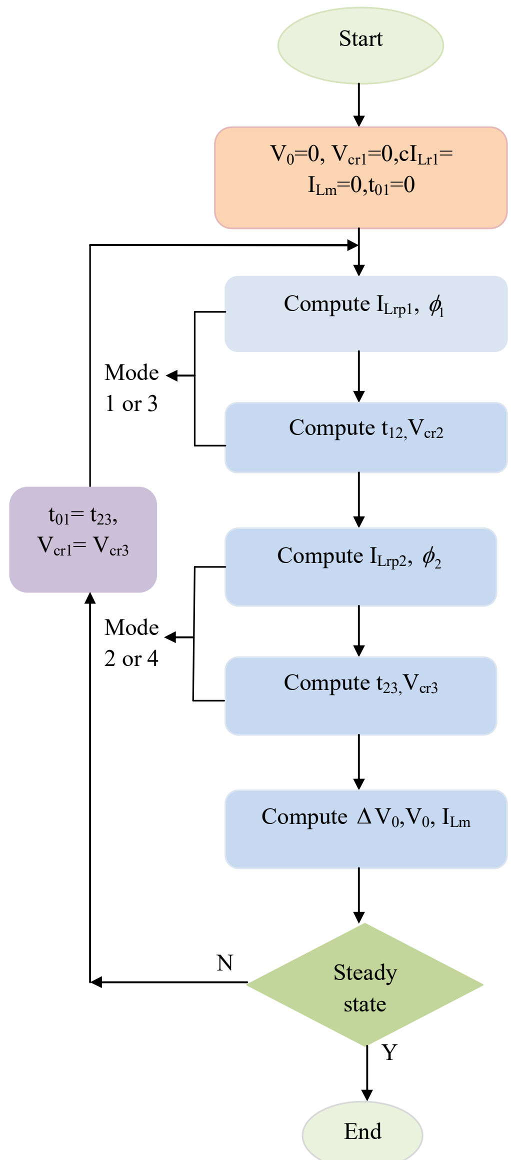

Fig. 2. *Flow chart of state variable measurement*

3.1.2 Resonant Current Peak Value

While the frequency of switching is lesser, the resonant current undergoes a value of peak that is like the resonant current amplitude, and it is like the value of resonant current for mode one and three while the frequency of switching is higher during the concluding stage. At the initial period, the voltage will be equal to zero at the output, hence $x_1 = x_4 = V_{in}, x_2 = x_3 = 0$, the modes introduced in this process decreases to two modes from four modes. In radian, as eq. (8), it states the trajectory of circular all through the complete model of the process; whereas, it states the resonant current at the concluding stage for every mode as $i_{Lr1}, i_{Lr2}, i_{Lr3}$, so forth. In eq. (8), f_n indicates the normalized frequency and $f_n = f/f_r$.

$$\alpha_1 = \omega_0 \frac{T_s}{2} = \frac{\pi}{f_n} \tag{10}$$

Actually, during the first switching duration, the resonant current's peak value is stated in Eq. (9), whereas V_{in} indicates the output voltage and R_1 indicates the input resistor.

$$I_{Lrm} = i_{Lr1} = \frac{R_1}{Z_0}\sin\left(\frac{\omega_0 T_s}{2}\right) = \frac{V_{in}}{Z_0}\sin\left(\frac{\pi}{f_n}\right)(f_n > 2) \tag{11}$$

Furthermore, it is identified that, $i_{Lr1} < \frac{R_1}{Z_0} < i_{Lr3} < i_{Lr2} < \frac{R_2}{Z_0}$, therefore eq. (10) and eq. (11) can be devised. In Eq. (11), θ_2 represents the vertex angle.

$$R_2 = 2R_1 \sin\left(\frac{\alpha_1}{2}\right) = 2V_{in}\sin\frac{\omega_0 T_s}{4} = 2V_{in}\sin\left(\frac{\pi}{2f_n}\right) \tag{12}$$

$$I_{Lrm} = i_{Lr2} = \frac{R_2}{Z_0}\sin(\alpha_1 - \theta_2) = \frac{R_2}{Z_0}\sin\left(\alpha_1 - \left(\frac{\pi}{2} - \frac{\alpha_1}{2}\right)\right) \tag{13}$$

$$I_{Lrm} = \frac{V_{in}}{Z_0}\sin\left(\frac{\pi}{f_n}\right) - \sin\left(\frac{2\pi}{f_n}\right) \quad (1.5 < f_n \le 2) \tag{14}$$

3.1.3 Optimizing frequency time constant

During the instant, while the state variables at the start-up course are deliberate, we attain the utmost resonant current value that can be illustrious with the attendance boundary to corroborate the converter factors. On the other hand, we can optimize the factors in order to assure the attendance restriction by iteration calculation. For the LLC converter by exact circuit factors operating with improved frequency technique, three qualities are frightening, the maximum resonant current value during the activation. Moreover, it needs the initial frequency, which suffices to oblige the limit of the current and considering the speed limit of circuit, controller and main driving switches. Generally, the final frequency can be fixed and it is close to the frequency of the steady-state. The stable time determining the frequency of switching with decreasing speed is vital and adaptable. However, a high time constant might reduce the LLC converter speed; as well it induces an extra period for settling to model the output voltage.

4. Stable LLC Converter using Black Widow Optimization Algorithm

4.1 Objective Model

The required voltage of the output is indicated by V_0^D and the required resonant current peak value is indicated by I_{Lrm}^D. For the output voltage, the error measurement e_1 is stated by eq. (13). Additionally, the error measurement e_2 for the resonant current peak value is stated by Eq. (14). Hence, as stated in eq. (15), the total error measurement can be estimated, whereas e^* the sum of the errors happens in the formative voltage of output and the resonant current peak value.

$$e_1 = \left(V_0^D - V_0\right) \tag{15}$$

$$e_1 = \left(I_{Lrm}^D - I_{Lrm}\right) \tag{16}$$

$$e^* = e_1 + e_2 \tag{17}$$

Therefore, the objective function of the proposed BWOA technique aspires to reduce the error model that is devised as stated in eq. (16).

$$G = \mathrm{Min}\left(e^*\right) \tag{18}$$

For solutions encoding, the solutions that is $C_{r,}$ $L_{r,}$ ϕ and τ are stated as input, whereas $L_{r,}$ states the inductor resonant, ϕ represent the initial point angle, $C_{r,}$ states the capacitor of the resonant and τ represents frequency time constant. For attaining the objective function, the solutions are encoded, which is reaching the least values of V_0 and I_{Lrm}. The upper and lower limits of C_r are 100e-6 and e-6. In the same way, the upper and lower limits of L_r are 5e-9 and e-9. The upper limits and lower limit of ϕ are e3 and 1 and the upper limits and lower limit of τ are 100 and 1 correspondingly.

4.2 Proposed BWOA Methodology

Fig. 3 demonstrates the flow chart of the adopted approach. Similar to conventional evolutionary approaches, the adopted approach begins by an initial spider's population, hence, every spider indicates a probable solution [15] [19].

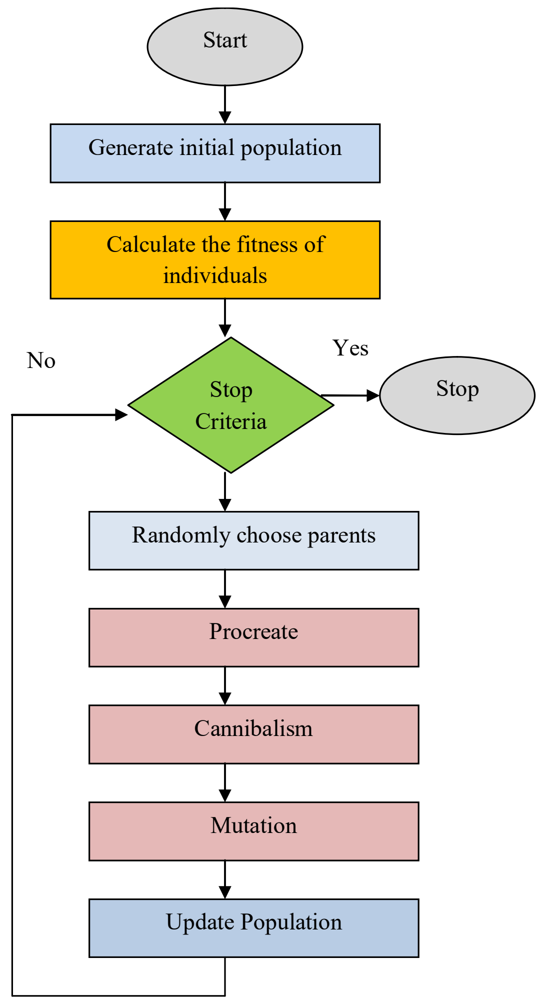

Fig. 3. *Flow chart of the proposed BWOA algorithm*

In pairs, these initial spiders decided to reproduce the new generation. After or during mating, the male black widow is eaten by the female. Subsequently, in her sperm thecae, she lifts saved sperms and liberates them into egg sacs. Since premature as eleven days subsequent to being laid, in the egg sacs, the spiderling appears. For numerous days, they live together on the parental web; the sibling cannibalism is discovered at that period. Subsequently, they take off by being driven on the wind.

4.2.1 Initial Population

With the intention to resolve an optimization issue, the problem of variables values should set up as a suitable framework for the present problem solution. In PSO [16] and GA [17] algorithms, this framework is named "Particle position" and "Chromosome", correspondingly, excluding here in BWOA it is named "widow". In BWOA, the probable solution to every issue has been dealt with as a Black widow spider. Every Black widow spider exhibits the issue variables values.

In a N_{var} – optimization issue, a widow represented as an array of $1 \times N_{var}$ indicating the issue solution and it is represented as below:

$$Widow = \left[y_1, y_2, ..., y_{N_{var}}\right] \tag{19}$$

Every variable value $\left(y_1, y_2, ..., y_{N_{var}}\right)$ indicates the floating-point number. The fitness of a widow is attained using assessment of fitness model f at a widow of $\left(y_1, y_2, ..., y_{N_{var}}\right)$. Consequently

$$fitness = f(widow) = f\left(y_1, y_2, ..., y_{N_{var}}\right) \tag{20}$$

A candidate widow matrix of size $N_{pop} \times N_{var}$ is created with an initial spider's population to establish the optimization approach. Subsequently, by mating, couples of parents arbitrarily are chosen to carry out the procreating model, in that the female black widow eats the male during or subsequent to that.

4.2.2 Procreate

As the pairs are self-governing of each other, they begin to mate with the intention of reproducing the novel generation, in correspond, naturally, every couple mate in its web, independently from the alternatives. In each mating, almost a thousand eggs are generated in the real world; however, ultimately, a few of the spider babies are sustained that are burly. At the present, here in this approach with the intention of reproducing, an array named alpha must further be produced providing widow array with arbitrary numbers comprising, after that offspring is generated by exploiting α with the subsequent to eq. 21 in that y_1 and y_2 are parents z_1 and z_2 are offspring.

$$\begin{cases} z_1 = \alpha \times y_1 + (1-\alpha) \times y_2 \\ z_2 = \alpha \times y_2 + (1-\alpha) \times y_1 \end{cases} \tag{21}$$

This procedure is reiterated for $N_{var}/2$, when arbitrarily chosen numbers must not be reproduced. Ultimately, the mother and children are continued as an array and categorized using their fitness function, at the present consistent with cannibalism rating; a few of the optimal individuals are included in the recently produced population. These steps give to all couples.

4.2.3 Cannibalism

Here, 3 categories of cannibalism are present. The initial one is sexual cannibalism [18], in that during or subsequent to mating, the male black widow is eaten by the female. In this approach, recognize the male and female can be recognized using their fitness values.

One more category is sibling cannibalism in that the burly spiderlings consume their smaller siblings. In this approach, a CR is set consistent with that the survivor's number is decided. In a few scenarios, the third categories of cannibalism are frequently experiential in that the child spiders consume their mother. To determine burly or weak spiderlings, the fitness value is exploited.

4.2.4 Mutation

In this phase, $Mute_{pop}$ indicates the number of individuals is selected randomly from the population. As Fig. 4 shows, in the array, each selected solution arbitrarily swaps two elements. Using the mutation rate the $Mute_{pop}$ is computed.

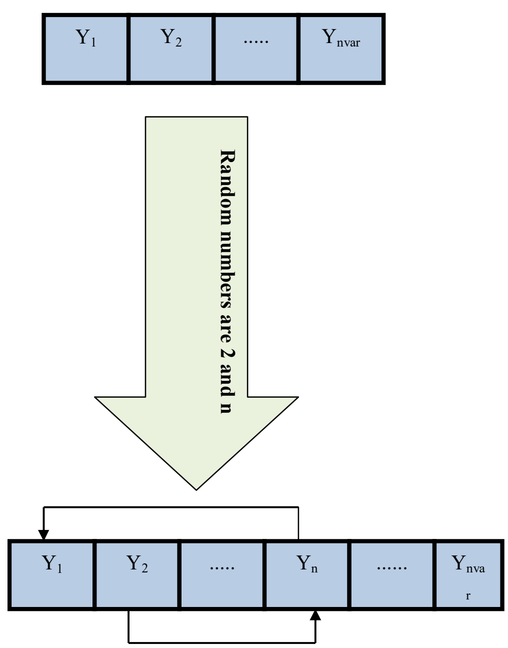

Fig. 4. *Diagrammatic representation of mutation*

4.2.5 Convergence

Similar to other evolutionary approaches, three-stop situations can be dealt with: i) a predefined number of iterations, ii) for some iterations, compliance of no alter in the value of the fitness for the optimal widow, iii) attaining to the particular level of accurateness.

5. Results and Discussions

5.1. Experimental Procedure

The proposed approach for LCC-RC has experimented in "MATLAB", and the best outcomes were attained. The parameters like V_0 and I_{Lrm} were tested in this experimentation. It was verified for three diverse simulations by setting the set points of (I_{Lrm}, V_0) at (15, 23), (5, 20) and (10, 25), correspondingly. The simulations were evaluated with the existing techniques, and the results have experimented.

5.2. Performance Analysis

For LCC-RC, the proposed method is evaluated for attaining the several parameters like rise time, settling maximum, settling minimum, undershoot, overshoot, peak, settling time, and peak time for 2 sets of simulations for I_{Lrm} and V_0 are performed for 3 setpoints like, (5, 20), (10, 25) and (15, 23). From Table 1, 2,3,4,5 and 6 for experiment one, two and three is conducted. Here, the adopted technique is better than conventional techniques like PSO, ABC, GWO, and FF algorithms.

Table 1. *Analysis of steady-state for I_{Lrm} of the first experiment*

Techniques	ABCPO	FFPO	PSOPO	GWOPO	Proposed algorithm
Rise time	0	0	0	0	0
Settling Min	15.19063	1.506247	3.902498	5.111981	5.012178
Settling Time	7.779576	6.371086	23.71366	8.557208	8.555614
Settling Max	18.57222	74.93567	22.83132	24.59467	24.30701
Undershoot	74.29702	20.42285	0	0	0
Overshoot	20.57158	501.9619	485.0438	63.96446	62.73971
Peak	18.57222	74.93567	22.83132	24.59467	24.10701
Peak Time	6	3	3	3	3

Table 2. *Analysis of steady-state for V_0 of the first experiment*

Techniques	ABCPO	FFPO	PSOPO	GWOPO	Proposed algorithm
Rise time	0	0	0	0	0
Settling Min	22.50717	14.03174	18.54166	22.48852	22.46603
Settling Time	4.512533	7.12522	26.10274	3.065112	3.107312
Settling Max	23.2531	33.48649	20.52631	22.98853	22.9805
Undershoot	0	0	0	0	0
Overshoot	0.001192	61.10978	0	0.106135	0.117007
Peak	23.2531	33.48649	20.52631	22.98853	22.9005
Peak Time	12	2	100	6	6.1

Table 3. *Analysis of steady-state for I_{Lrm} of the second experiment*

Techniques	ABCPO	FFPO	PSOPO	GWOPO	Proposed algorithm
Rise time	0	0	0	0	0
Settling Min	5.250561	4.997268	4.285375	4.999946	5.010397
Settling Time	12.65921	18.01649	24.78616	13.77991	13.76682
Settling Max	34.28264	26.51892	20.06399	32.70482	32.76768
Undershoot	3.117753	0	0	1.833235	1.824594
Overshoot	552.9328	430.6683	368.1968	554.1035	554.1317
Peak	34.28264	26.51892	20.06399	32.70482	32.71668
Peak Time	3	3	3	3	3

Table 4. *Analysis of steady-state for V_0 of the second experiment*

Techniques	ABCPO	FFPO	PSOPO	GWOPO	Proposed algorithm
Rise time	0	0	0	0	0
Settling Min	18.59842	18.89421	19.03922	18.64038	18.62128
Settling Time	11.75384	17.8867	25.88162	13.15562	13.13255
Settling Max	20.17241	20.96248	21.02916	20.17241	20.14241
Undershoot	0	0	0	0	0
Overshoot	0	0	0	0	0
Peak	20.17241	20.96248	21.02916	20.17241	20.13241
Peak Time	100	100	100	100	100

Table 5. *Analysis of steady-state for I_{Lrm} for the third experiment*

Techniques	ABCPO	FFPO	PSOPO	GWOPO	Proposed algorithm
Rise time	0	0	0	0	0
Settling Time	8.459763	7.482513	23.71366	13.16852	13.06433
Settling Time	8.459763	7.482513	23.71366	13.16852	13.06433
Settling Max	37.80458	62.32365	22.83132	16.78018	16.77473
Undershoot	0	95.81646	0	0	0
Overshoot	273.1331	523.2078	485.0438	67.80226	67.58612
Peak	37.80458	62.32365	22.83132	16.78018	16.77473
Peak Time	3	3	3	6	6

Table 6. *Analysis of steady-state for V_0 for the third experiment*

Techniques	ABCPO	PSOPO	FFPO	GWOPO	Proposed algorithm
Rise time	0	0	0	0	0
Settling Min	20.25554	18.54166	20.18556	20.76239	20.7883
Settling Time	5.911161	26.10274	3.369537	9.029978	8.951225
Settling Max	22.1793	20.52631	21.8122	22.72726	22.71152
Undershoot	0	0	0	0	0
Overshoot	$7.29e^{-09}$	0	6.009367	0	0
Peak	22.1793	20.52631	21.8122	22.72726	22.71052
Peak Time	29	100	2	76	74

6. Conclusion

Recently, the LLC RC was extensively exploited in DC-DC conversion technologies. Nevertheless, the LLC RC parasitic modules had an important effect in sensible applications, like the soft-switching of power devices and power on the loss of the conduction, the voltage oscillation across rectifier diodes, at light load condition the unregulated output voltage and etc. In this work, improved LLC-RC using optimizing the resonant inductor current and output voltage by exploiting the BWO approach which can reduce the system error was proposed. The proposed BWOA was proposed in order to update the enhanced model for the optimization reason. Furthermore, the algorithm was evaluated with conventional algorithms via the analysis of the error, steady-state, and stability. From the experimentation outcomes, the performance ability of the proposed BWOA on the basis of the LLC-RC was scientifically established.

Compliance with Ethical Standards

Conflicts of interest: Authors declared that they have no conflict of interest.

Human participants: The conducted research follows the ethical standards and the authors ensured that they have not conducted any studies with human participants or animals.

References

[1] Siniša Zorica, Marko Vukšić, Tihomir Betti,"Design considerations of the multi-resonant converter as a constant current source for electrolyser utilisation", International Journal of Electrical Power & Energy Systems, Volume 111, October 2019, Pages 237-247.

[2] Chuang Liu, Xuejiao Li, Yuemei Zhi, Guowei Cai,"New breed of solid-state transformer mainly combing hybrid cascaded multilevel converter with resonant DC-DC converters",Applied Energy, Volume 210, 15 January 2018, Pages 724-736.

[3] Chih-Chiang Hua, Yung-Lin Deng,"A Novel Dual-Bridge LLC Resonant Converter with Wide Range of Low Input Voltage", Energy Procedia, Volume 156, January 2019, Pages 361-365

[4] Dongjiang Yang, Bin Duan, Wenlong Ding, Jinqiu Song, Chenghui Zhang,"A bidirectional LLC-C Resonant DC-DC Converter Based on Normalized Symmetry Resonant Tank", IFAC-PapersOnLine, Volume 51, Issue 31, 2018, Pages 685-689.

[5] Li, Fang Hao, Ruixiang Lei, Haodong Zhang, Xinyi You, Xiaojie. The Influence of Parasitic Components on LLC Resonant Converter. Energies. 12. 4305, 2019.

[6] Arief Noor Rahman, Cheng- Yan Lee, Huang-Jen Chiu,Yao-Ching Hsieh, "Bidirectional Three-Phase LLC Resonant Converter",IEEE Transportation Electrification Conference and Expo, Asia-Pacific (ITEC Asia-Pacific), 2018.

[7] S. De Simone, C. Adragna, C. Spini, and G. Gattavari, “Design-oriented Steady-state analysis of LLC resonant converters based on FHA,” in Proc. Int. Symp. Power Electron. Elect. Drives, Autom. Motion, pp. 200–207, 2006.

[8] B. Lu, W. Liu, Y. Liang, F. C. Lee, and J. D. Van Wyk, “Optimal design methodology for LLC resonant converter,” in Proc. Appl. Power Electron.Conf. Expo., pp. 533–538, 2006.

[9] T. Liu, Z. Zhou, A. Xiong, J. Zeng, and J. Ying, “A novel precise design method for LLC series resonant converter,” in Proc. Int. Telecommun.Energy Conf., pp. 1–6, 2006.

[10] X. Xie, J. Zhang, C. Zhao, Z. Zhao, and Z. Qian, “Analysis and optimization of LLC resonant converter with a novel over-current protection circuit,” IEEE Trans. Power Electron., vol. 22, no. 2, pp. 435–443, March 2007.

[11] H.-S. Choi, “Design consideration of half-bridge LLC resonant converter,”J. Power Electron., Volume. 7, issue. 1, page no. 13–20, 2007.

[12] X. Fang, H. Hu, F. Chen, U. Somani, E.Auadisian, J. Shen, and I. Batarseh,“Efficiency-oriented optimal design of the LLC resonant converter based on peak gain placement,” IEEE Trans. Power Electron., Volume. 28, issue. 5, page no. 2285–2296, May 2013.

[13] F. Musavi,M. Craciun, D. S. Gautam,W. Eberle, andW. G. Dunford, “An LLC resonant DC-DC converter for wide output voltage range battery charging applications,” IEEE Trans. Power Electron., Volume. 28, issue. 12, page no. 5437–5445, Dec. 2013.

[14] H. Wang, Y. Chen, Y. F. Liu, J. Afsharian and Z. Yang, "A Passive Current Sharing Method With Common Inductor Multiphase LLC Resonant Converter,"IEEE Transactions on Power Electronics, Volume. 32, issue. 9, page no. 6994-7010, Sept. 2017.

[15] Vahideh Hayyolalam, Ali Asghar Pourhaji Kazem,"Black Widow Optimization Algorithm: A novel meta-heuristic approach for solving engineering optimization problems",Engineering Applications of Artificial Intelligence, Volume 87, January 2020.

[16] He, Qie, Wang, Ling,. An effective co-evolutionary particle swarm optimization for constrained engineering design problems. Eng. Appl. Artif. Intell. Issue no: 20 (1), 89–99, 2007.

[17] Abualigah, Laith Mohammad Qasim, Hanandeh, Essam S., Applying genetic algorithms to information retrieval using vector space model. Int. J. Comput. Sci., Eng. Appl. Issue no: 5 (1), 19, 2015.

[18] Elgar, Mark A., Nash, David R., Sexual cannibalism in the garden spider araneus diadematus. Anim. Behav. Issue no: 36 (5), 1511–1517, 1988.

[19] Scott, Catherine, Kirk, Devin, McCann, Sean, Gries, Gerhard, Web reduction by courting male black widows renders pheromone-emitting females’ webs less attractive to rival males. Anim. Behav. Volume 107, 71–78, July 2015.

[20] T.C.Subramanyam,S S Tulasi Ram and J B V Subrahmanyam,"HGAGWO: A Multi-Objective Optimal Positioning and Sizing of Fuel Cells in DG Systems",Journal of Computational Mechanics, Power System and Control (JCMPS), Volume 1, Issue 1, October 2018.